

## Supplementary Information

# **Dual-ion acceptable vanadium carbide nanowire cathode integrated with carbon clothes for long cycle stability**

Sanghee Nam<sup>a</sup>, Pitchai Thangasamy<sup>a</sup>, Saewoong Oh<sup>a</sup>, Manmatha Mahato<sup>a</sup>, Nikhil Koratkar<sup>b</sup>,

Il-Kwon Oh<sup>\*,a</sup>

<sup>a</sup> National Creative Research Initiative for Functionally Antagonistic Nano-Engineering, Department of Mechanical Engineering, Korea Advanced Institute of Science and Technology (KAIST), 291 Daehak-ro, Yuseong-gu, Daejeon 34141, Republic of Korea.

<sup>b</sup> Department of Mechanical, Aerospace and Nuclear Engineering, Rensselaer Polytechnic Institute, 110 8<sup>th</sup> Street, Troy, NY 12180, USA.

\* Corresponding author

Phone: +82-42-350-1520, Fax: +82-42-350-1510, e-mail: ikoh@kaist.ac.kr

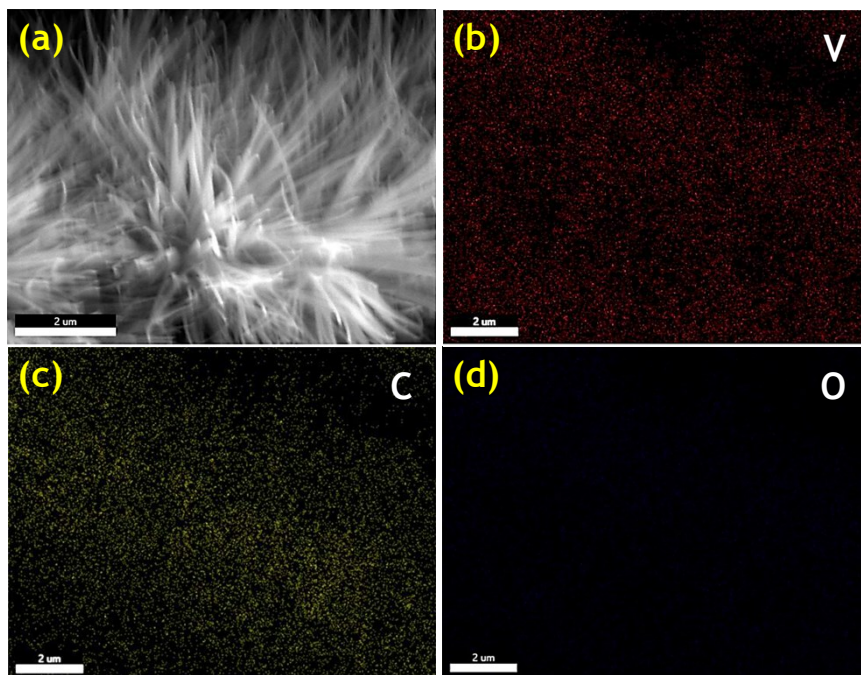


**Fig. S1.** Elemental study obtained with SEM EDS mapping.

**Elemental analysis for V, C and O of  $V_8C_7$  NWs**

**Table S1.** Elemental analysis for C and O in weight percent and V, C and O in atomic percent

Material	Chemical composition				
	wt%			at%	
	C	O	V	C	O
$V_8C_7$ NWs	16.94	0.42	53.1	38.4	8.5

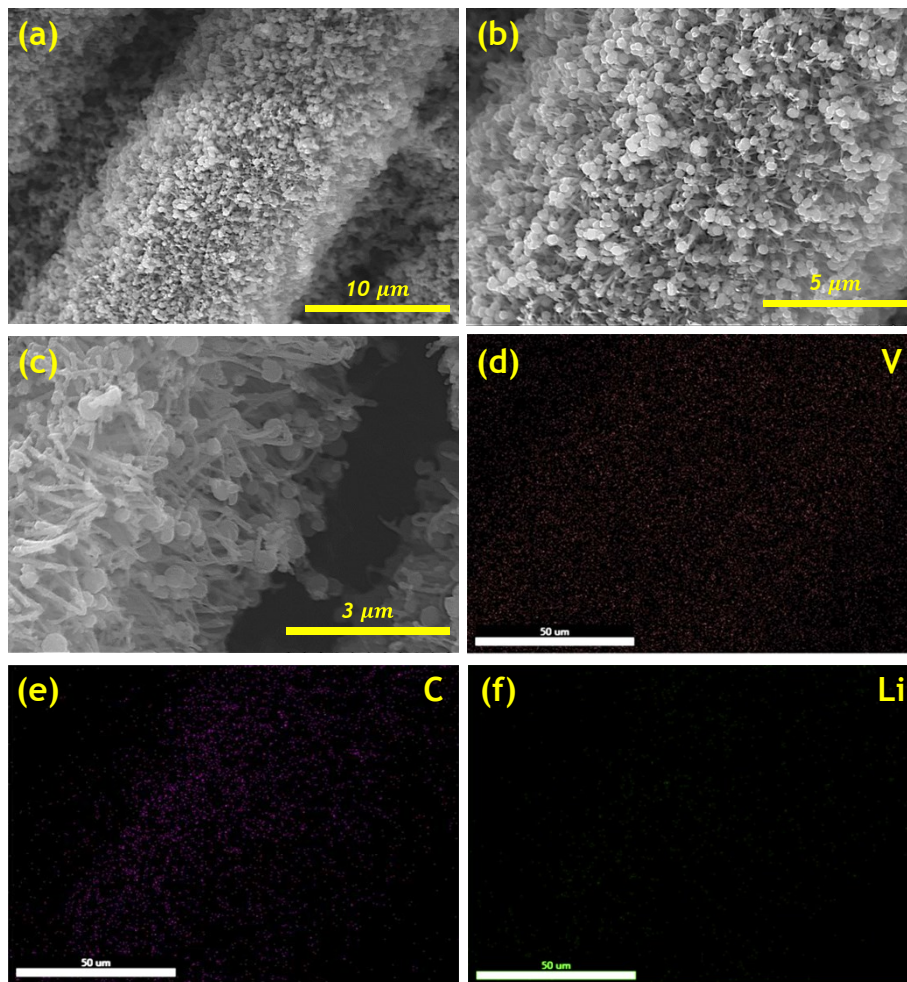


**Fig. S2.** Morphological change of  $V_8C_7$  NWs (a-d) and elemental analysis (e-h) after 10 cycle to charge and discharge.

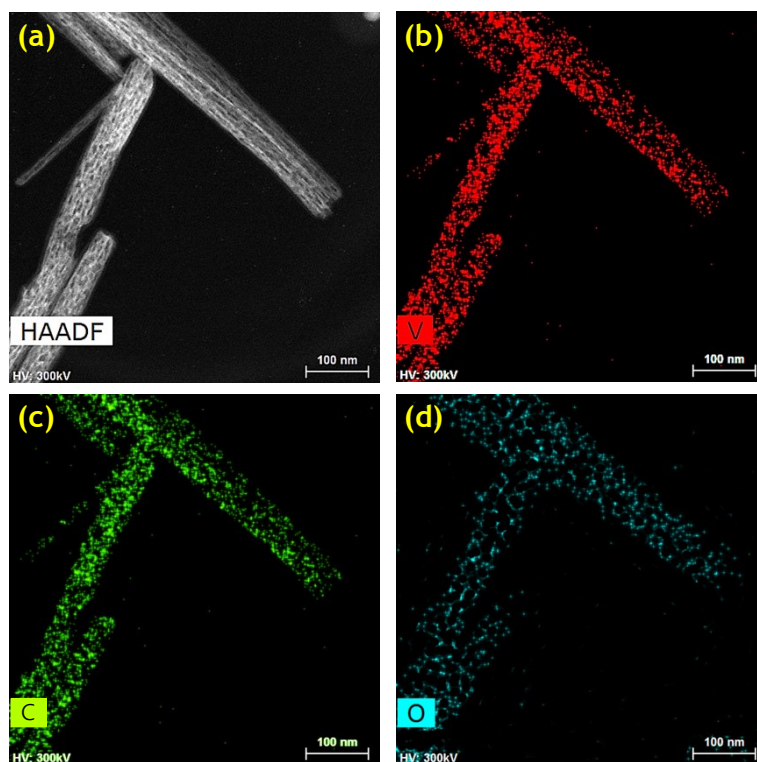


**Fig. S3.** Elemental study obtained with HAADF TEM EDS mapping.

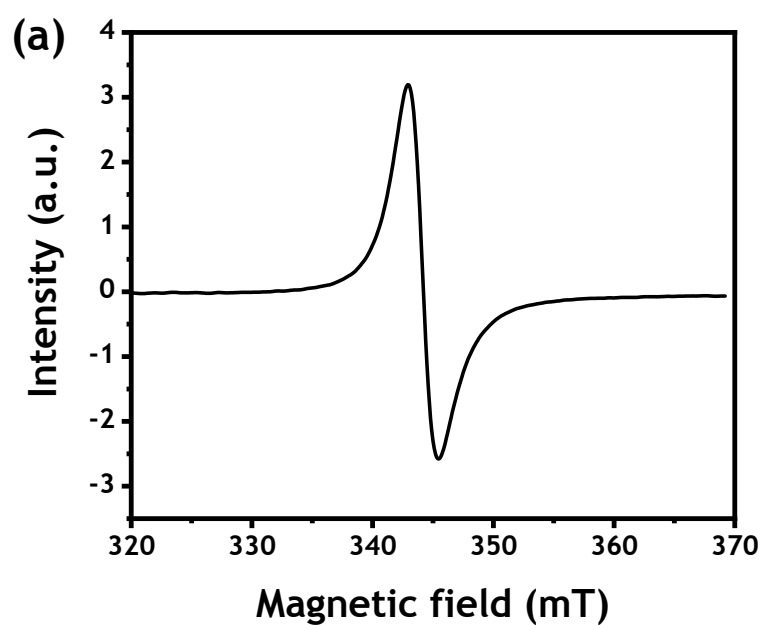
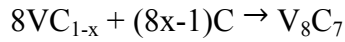
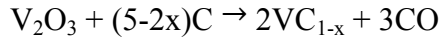
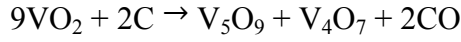


**Fig. S4.** Electron paramagnetic resonance study of  $V_8C_7$  NWs.

### Reaction equations in detail during synthesis of the $V_8C_7$ NWs from precursors.

The chemical reactions involved during ultra-sonication subject, hydrothermal synthesis and annealing process can be described as follows:



### Calculation for resistivity and electrical conductivity from sheet resistance measured.

$$\rho [\Omega \text{ cm}^{-1}] = R_s [\Omega \text{ sq}^{-1}] \times t [\text{cm}]$$

$$\sigma [S \text{ m}^{-1}] = \frac{1}{\rho}$$

where  $\rho$  is resistivity,  $\sigma$  is electrical conductivity,  $R_s$  is sheet resistance, and  $t$  is thickness of material.

Thickness of our materials were average  $150 \times 10^{-6}$  m.

**Table S2.** Sheet resistance and calculated electrical conductivity of  $V_8C_7$  NWs,  $V_2O_5$  NWs and other vanadium-based materials.

Material	Resistivity	Conductivity	Temperatur	Reference
----------	-------------	--------------	------------	-----------

			e	
			[K]	
$V_8C_7$ NWs	$15.54 \text{ m}\Omega \text{ cm}^{-1}$	$6.435 \times 10^3 \text{ S m}^{-1}$	RT	This work
	$26.22 \text{ m}\Omega \text{ cm}^{-1}$	$5.342 \times 10^3 \text{ S m}^{-1}$		
	$22.47 \text{ m}\Omega \text{ cm}^{-1}$	$5.565 \times 10^3 \text{ S m}^{-1}$		
	$22.89 \text{ m}\Omega \text{ cm}^{-1}$	$5.921 \times 10^3 \text{ S m}^{-1}$		
$V_2O_3$ NWs	$32.09 \text{ m}\Omega \text{ cm}^{-1}$	$3.116 \times 10^3 \text{ S m}^{-1}$	RT	This work
	$32.06 \text{ m}\Omega \text{ cm}^{-1}$	$3.119 \times 10^3 \text{ S m}^{-1}$		
	$32.08 \text{ m}\Omega \text{ cm}^{-1}$	$3.117 \times 10^3 \text{ S m}^{-1}$		
	$32.10 \text{ m}\Omega \text{ cm}^{-1}$	$3.115 \times 10^3 \text{ S m}^{-1}$		
$V_2O_5$ NWs	$37.32 \Omega \text{ cm}^{-1}$	$4.019 \times 10^1 \text{ S m}^{-1}$	RT	This work
	$37.20 \Omega \text{ cm}^{-1}$	$4.032 \times 10^1 \text{ S m}^{-1}$		
	$37.26 \Omega \text{ cm}^{-1}$	$4.027 \times 10^1 \text{ S m}^{-1}$		
	$37.38 \Omega \text{ cm}^{-1}$	$4.013 \times 10^1 \text{ S m}^{-1}$		
$V_8C_7$	$3.2 \mu\Omega \text{ cm}^{-1}$	-	1,378.15 K	[1]
Ordered $V_8C_7$	$30 \mu\Omega \text{ cm}^{-1}$	-	RT	[1]
Annealed $V_8C_7$	$40 \mu\Omega \text{ cm}^{-1}$	-	RT	[1]
Disordered $V_8C_7$	$49 \mu\Omega \text{ cm}^{-1}$	-	RT	[1]
Quenched $V_8C_7$	$70 \mu\Omega \text{ cm}^{-1}$	-	RT	[1]
$V_2O_3$ nanosheet	-	$2.500 \times 10^1 \text{ S m}^{-1}$	RT	[2]
$VO_2$	-	$1.000 \times 10^2 \text{ S m}^{-1}$	340 K	[3]

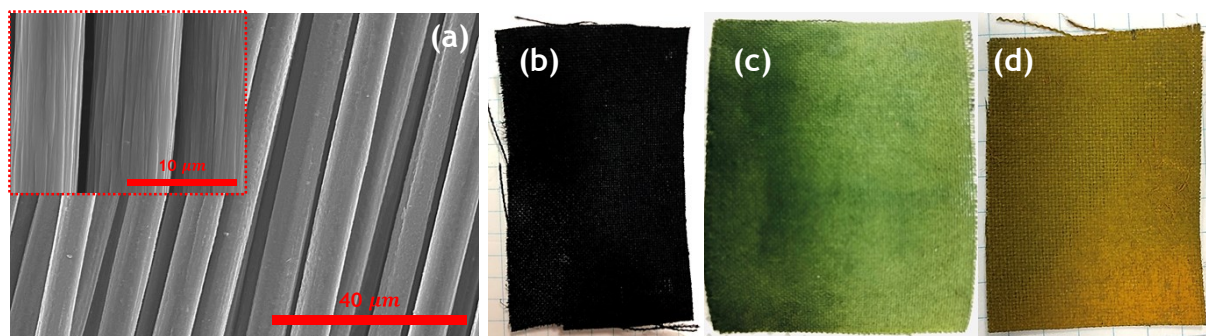


**Fig. S5.** (a) SEM images of bare carbon clothes, (b)  $V_8C_7$  NWs, (c)  $V_2O_3$  NWs, and (d)  $V_2O_5$  NWs grown on the carbon clothes.

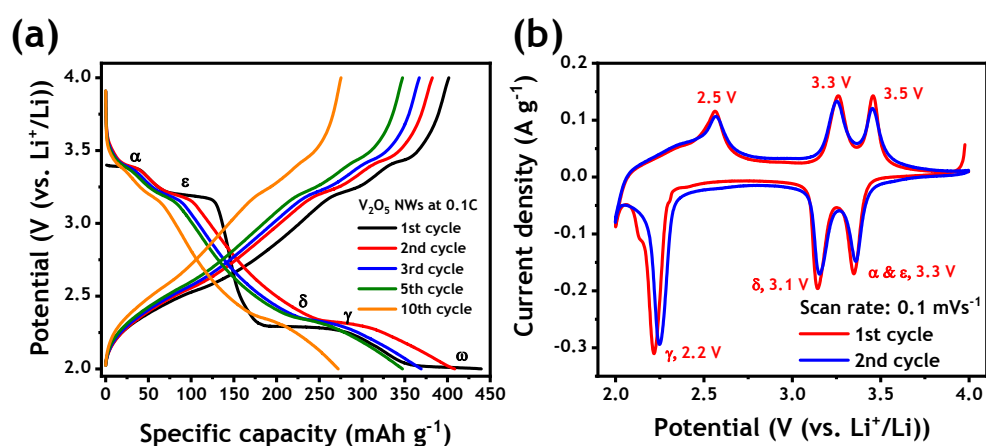


**Fig. S6.** Charge-Discharge curves (a) and CV measurement (b) of  $V_2O_5$  NWs for LIBs.

**Table S3.** The list of other vanadium compounds in the potential window between 2 and 4 V (vs.  $Li^+/Li$ ).

Material	Specific capacity [mAh g <sup>-1</sup> ]	Cycle number	Capacity fading per cycle [%]	Current density [mA g <sup>-1</sup> ]	Referenc e
$V_8C_7$ Nanowires	303	200	0.4	30	This work
1D nanostructure	312	20	1.4	50	[4]
1D nanorods	274	30	0.6	15	[5]
1D nanorods	288	50	0.18	10	[6]
3D uniform yolk-shell microspheres	280	30	0.7	30	[7]
2D self-assembled nanobelt membrane	290	50	0.28	500	[8]
2D porous nanostructured films	294	40	0.45	300	[9]
3D hierarchical urchin-like microflowers	274	50	0.4	300	[10]
3D nanostructured hollow	241	110	0.191	300	[11]

microspheres					
3D hollow microspheres	256	50	0.22	300	[12]
2D leaf-like nanosheets	264	100	0.22	500	[13]
3D hierarchical microspheres	266	100	0.25	300	[14]
3D yolk-shell powders	271	100	0.26	1,000	[15]

---

## References

- [1] Shacklette LW, Williams WS. Influence of order-disorder transformations on the electrical resistivity of vanadium carbide. *Phys Rev B* 1973;7:5041–53.
- [2] Li Q, Xue Y, Qian Y. V<sub>2</sub>O<sub>3</sub> ultrathin nanosheets: Controlled synthesis and electrical properties. *Mater Lett* 2014;130:198–201.
- [3] Andreev VN, Klimov VA. Electrical conductivity of the semiconducting phase in vanadium dioxide single crystals. *Phys Solid State* 2007;49:2251–5.
- [4] Ng SH, Chew SY, Wang J, Wexler D, Tournayre Y, Konstantinov K, et al. Synthesis and electrochemical properties of V<sub>2</sub>O<sub>5</sub> nanostructures prepared via a precipitation process for lithium-ion battery cathodes. *J Power Sources* 2007;174:1032–5.
- [5] Pan A, Zhang JG, Nie Z, Cao G, Arey BW, Li G, et al. Facile synthesized nanorod structured vanadium pentoxide for high-rate lithium batteries. *J Mater Chem* 2010;20:9193–9.
- [6] Shao J, Li X, Wan Z, Zhang L, Ding Y, Zhang L, et al. Low-cost synthesis of hierarchical V<sub>2</sub>O<sub>5</sub> microspheres as high-performance cathode for lithium-ion batteries. *ACS Appl Mater Interfaces* 2013;5:7671–5.
- [7] Ko YN, Kang YC, Park S Bin. A new strategy for synthesizing yolk-shell V<sub>2</sub>O<sub>5</sub>

- powders with low melting temperature for high performance Li-ion batteries. *Nanoscale* 2013;5:8899–903.
- [8] Glushenkov AM, Hassan MF, Stukachev VI, Guo Z, Liu HK, Kuvshinov GG, et al. Growth of  $V_2O_5$  nanorods from ball-milled powders and their performance in cathodes and anodes of lithium-ion batteries. *J Solid State Electrochem* 2010;14:1841–6.
- [9] Liu J, Zhou Y, Wang J, Pan Y, Xue D. Template-free solvothermal synthesis of yolk-shell  $V_2O_5$  microspheres as cathode materials for Li-ion batteries. *Chem Commun* 2011;47:10380–2.
- [10] Wang Y, Zhang HJ, Siah KW, Wong CC, Lin J, Borgna A. One pot synthesis of self-assembled  $V_2O_5$  nanobelt membrane via capsule-like hydrated precursor as improved cathode for Li-ion battery. *J Mater Chem* 2011;21:10336–41.
- [11] Liu Y, Li J, Zhang Q, Zhou N, Uchaker E, Cao G. Porous nanostructured  $V_2O_5$  film electrode with excellent Li-ion intercalation properties. *Electrochem Commun* 2011;13:1276–9.
- [12] Pan A, Wu H Bin, Yu L, Zhu T, Lou XW. Synthesis of hierarchical three-dimensional vanadium oxide microstructures as high-capacity cathode materials for lithium-ion batteries. *ACS Appl Mater Interfaces* 2012;4:3874–9.
- [13] Uchaker E, Zhou N, Li Y, Cao G. Polyol-mediated solvothermal synthesis and electrochemical performance of nanostructured  $V_2O_5$  hollow microspheres. *J Phys Chem C* 2013;117:1621–6.
- [14] Pan A, Wu H Bin, Yu L, Lou XWD. Template-Free Synthesis of  $VO_2$  Hollow Microspheres with Various Interiors and Their Conversion into  $V_2O_5$  for Lithium-Ion

Batteries. *Angew Chemie* 2013;125:2282–6.

- [15] Li Y, Yao J, Uchaker E, Yang J, Huang Y, Zhang M, et al. Leaf-like  $V_2O_5$  nanosheets fabricated by a facile green approach as high energy cathode material for lithium-ion batteries. *Adv Energy Mater* 2013;3:1171–5.